

# A Conformational Switch Triggers Nitrogenase Protection from Oxygen Damage by Shethna Protein II (FeSII)

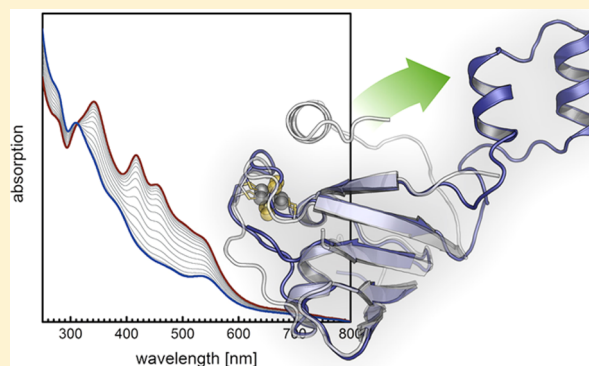
Julia Schlesier,<sup>†</sup> Michael Rohde,<sup>†</sup> Stefan Gerhardt,<sup>†</sup> and Oliver Einsle<sup>\*,†,‡</sup>

<sup>†</sup>Institute for Biochemistry, Albert-Ludwigs-Universität Freiburg, Albertstrasse 21, 79104 Freiburg, Germany

<sup>‡</sup>BIOSS Centre for Biological Signalling Studies, Schänzlestr.1, 79104 Freiburg, Germany

**S** Supporting Information

**ABSTRACT:** The two-component metalloprotein nitrogenase catalyzes the reductive fixation of atmospheric dinitrogen into bioavailable ammonium in diazotrophic prokaryotes. The process requires an efficient energy metabolism, so that although the metal clusters of nitrogenase rapidly decompose in the presence of dioxygen, many free-living diazotrophs are obligate aerobes. In order to retain the functionality of the nitrogen-fixing enzyme, some of these are able to rapidly “switch-off” nitrogenase, by shifting the enzyme into an inactive but oxygen-tolerant state. Under these conditions the two components of nitrogenase form a stable, ternary complex with a small [2Fe:2S] ferredoxin termed FeSII or the “Shethna protein II”. Here we have produced and isolated *Azotobacter vinelandii* FeS II and have determined its three-dimensional structure to 2.1 Å resolution by X-ray diffraction. In the crystals, the dimeric protein was present in two distinct states that differ in the conformation of an extended loop in close proximity to the iron–sulfur cluster. We show that this rearrangement is redox-dependent and forms the molecular basis for oxygen-dependent conformational protection of nitrogenase. Protection assays highlight that FeSII binds to a preformed complex of MoFe and Fe protein upon activation, primarily through electrostatic interactions. The surface properties and known complexes of nitrogenase component proteins allow us to propose a model of the conformationally protected ternary complex of nitrogenase.

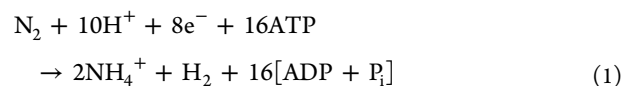


## INTRODUCTION

Although dinitrogen gas ( $N_2$ ) is the main constituent of Earth’s atmosphere, the extraordinary stability of the triple-bonded molecule makes it a global sink for the element that at any given time contains an estimated 99% of all [N] cycling through the biosphere.<sup>1</sup> While this stability makes  $N_2$  a highly suited end-product of different metabolic pathways, evolution according to current knowledge has brought forth only a single enzyme system—nitrogenase—that is able to tap into the vast atmospheric reservoir.<sup>2</sup> It breaks the  $N_2$  triple bond and produces the reduced modification of ammonium ( $NH_4^+$ ) that is readily bioavailable through incorporation into glutamine or glutamate. Prokaryotes that have the ability to reductively fix dinitrogen are classified as *diazotrophs*, and they accordingly play a key role in the global ecosystem. Leguminous and few other plants have learned to gain access to nitrogen through an intricate symbiosis with specific diazotrophs. This involves the formation of root nodules; specialized plant organs populated by the bacteria that provide ammonium to the plant in return for photosynthetically generated sugars as an energy source.<sup>3</sup> They also provide an efficient protection from dioxygen ( $O_2$ ) that is highly detrimental for the metal clusters of the nitrogenase system. Most diazotrophs, however, are free-living marine or soil organisms that not only cope with atmospheric

$O_2$ , but that are even dependent on its presence, as the high energy requirements for fixing nitrogen force them into an obligate aerobic lifestyle. This has given rise to what Postgate has termed the “oxygen problem” of biological nitrogen fixation.<sup>4–6</sup> In free-living diazotrophs such as *Azotobacter*, two key mechanisms serve to protect nitrogenase. First, the high respiratory activity of multiple types of oxidases is sufficient to effectively keep the cytoplasm—where nitrogenase is located—in a nearly anoxic state. This *respiratory protection* is complemented by a *conformational protection* (or “switch-off” reaction), where the component proteins of nitrogenase rapidly attain an inactive, but oxygen-tolerant state that allows them to survive limited periods of oxygen stress.<sup>7</sup>

Nitrogenase is a complex metalloprotein consisting of two distinct component proteins that interact dynamically to catalyze the reaction



Received: October 3, 2015

Published: December 11, 2015

so that for the reduction of a single molecule of  $N_2$  at least 16 ATP are hydrolyzed and  $H_2$ —at variable stoichiometries—is generated.<sup>8</sup> ATP binding and hydrolysis occurs on one component of nitrogenase, the Fe protein (or dinitrogenase reductase). Fe protein is a homodimeric protein of 60 kDa belonging to the family of P-loop NTPases that couple the hydrolysis of nucleoside triphosphates to a conformational change in two conserved loop regions termed Switch I and Switch II. Fe protein furthermore contains a cubane-type  $[4Fe:4S]$  cluster bridging the two subunits.<sup>9</sup> In synchrony with ATP hydrolysis, this cluster is the only known means of transferring electrons to the second, catalytic component of nitrogenase that is functional in supporting dinitrogen reduction. Catalysis of all known substrates of nitrogenase occurs on the second component, MoFe protein or dinitrogenase.<sup>10–12</sup> This 230 kDa  $\alpha_2\beta_2$ -heterotetramer contains two large iron–sulfur clusters in each  $\alpha\beta$ -unit. Electrons from Fe protein first reach P-cluster, an  $[8Fe:7S]$  moiety that serves as electron relay to the second metal site, FeMo cofactor, where catalysis takes place. With a composition of  $[Mo:7Fe:9S:C]:$ homocitrate, FeMo cofactor is the largest and most complex bioinorganic metal cluster known to date, and its exact catalytic functionality remains to be fully elucidated.<sup>13</sup> When the nitrogenase system is operational, the transfer of each single electron from Fe protein to MoFe protein sequentially involves the binding of 2 molecules of ATP to Fe protein, reduction of the  $[4Fe:4S]$  cluster in Fe protein, and the formation of a complex between both protein components. ATP is then hydrolyzed, triggering the transfer of an electron from P-cluster to FeMo cofactor, followed by the oxidation of Fe protein and its dissociation from MoFe protein. This cycle is repeated at least eight times for one complete turnover of  $N_2$ , depending on the stoichiometry of  $H_2$  evolution. For the conformational protection of this dynamic system during the oxygen-induced switch-off in *A. vinelandii*, Robson and Postgate identified an additional component, FeSII or the “Shethna Protein II” that is able to form a protective complex of all three proteins.<sup>4,14</sup> This complex could be isolated, its formation was reversible,<sup>15,16</sup> and *A. vinelandii* FeSII produced recombinantly in *Escherichia coli* had a significant oxygen-protective effect on the isolated components of the nitrogenase system in vitro.<sup>17</sup> FeSII is a small (12 kDa) homodimeric ferredoxin containing a single  $[2Fe:2S]$  cluster per monomer. Low-temperature resonance Raman spectroscopy indicated that the cluster was not solvent-exposed and its midpoint redox potential was determined by EPR-monitored, dye-mediated redox titration to  $-262$  mV at pH 7.0. Crystals of recombinant FeSII belonging to an orthorhombic space group were also shown,<sup>17</sup> but to date no three-dimensional structure is available.

In order to elucidate the molecular basis for the nitrogenase switch-off reaction we produced recombinant *A. vinelandii* FeSII, crystallized the protein and solved its structure by single-wavelength anomalous dispersion. In the crystal we observe two distinct conformations that suggest a redox-dependent activation mechanism with obvious implications for the mechanism of conformational protection of nitrogenase.

## RESULTS

**Protection of Nitrogenase by FeSII.** The Shethna Protein FeSII was initially produced with the addition of a C-terminal hexahistidine affinity tag for purification by immobilized metal-ion affinity chromatography. However, while the tagged protein could be purified to homogeneity with an intact  $[2Fe:2S]$

cluster, no protection of nitrogenase during oxygen exposure was detected (data not shown). We therefore altered the expression construct to produce an untagged variant that was subsequently isolated by cation exchange chromatography. This form of FeSII was then investigated for its ability to protect isolated nitrogenase from transient exposure to oxygen. To a reaction mixture containing ATP and an ATP-regenerating system (phosphocreatine and phosphocreatine kinase) we added MoFe and Fe proteins separately or together and assayed in the absence and presence of FeSII, respectively. The mixture was sealed in a Wheaton vial and the gas space was exchanged for 98% Ar, 2%  $O_2$  for varying amounts of time. After removal of  $O_2$  by flushing and addition of the respective missing component protein and the reductant  $Na_2S_2O_4$ , the acetylene-reducing activity was determined. In line with earlier studies we find that MoFe protein alone is moderately  $O_2$ -sensitive, retaining 80% of its activity after 30 min exposure to a 2%  $O_2$  atmosphere (Figure 1A).<sup>7</sup>

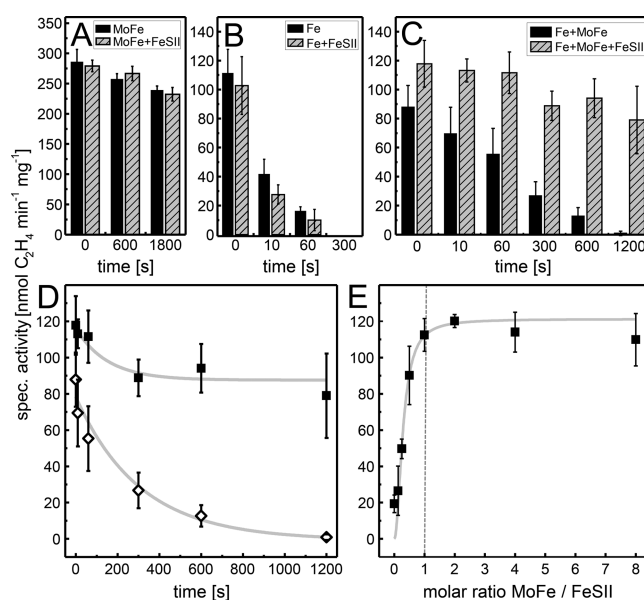


**Figure 1.** Protective effect of FeSII on nitrogenase activity. (A) Exposure of MoFe protein to 2%  $O_2$  prior to an activity assay after  $O_2$  removal. The protein loses activity very slowly, independent of the presence of FeSII. (B) In the same type of assay, Fe protein is rapidly inactivated and FeSII offers no protection. (C) Combining both components before  $O_2$  exposure leads to stabilization per se that is strongly enhanced through FeSII. (D) Time course of  $O_2$  exposure of both component proteins. In the absence ( $\diamond$ ) of stoichiometric amounts of FeSII activity is lost after 20 min, while in the presence ( $\blacksquare$ ) of the FeSII protein 70% activity are retained. (E) Titration of components. Full protection is achieved at a stoichiometric ratio of 1 FeSII dimer per MoFe heterotetramer.

In contrast, Fe protein rapidly loses its functionality with a  $t_{1/2}$  below 10s (Figure 1B). Neither component protein was stabilized by the addition of FeSII. This changed when both parts of the nitrogenase system were combined in the mixture before oxygen exposure (Figure 1C). Even in the absence of FeSII, activity was lost only after 20 min of exposure to 2%  $O_2$ , underlining that the presence of MoFe protein alone is sufficient to extend the survival time of Fe protein by at least an order of magnitude. Under anoxic conditions, the addition of FeSII had no effect on activity, as it remains in an inactive state that does not interfere with nitrogenase catalysis (Figure 1A,

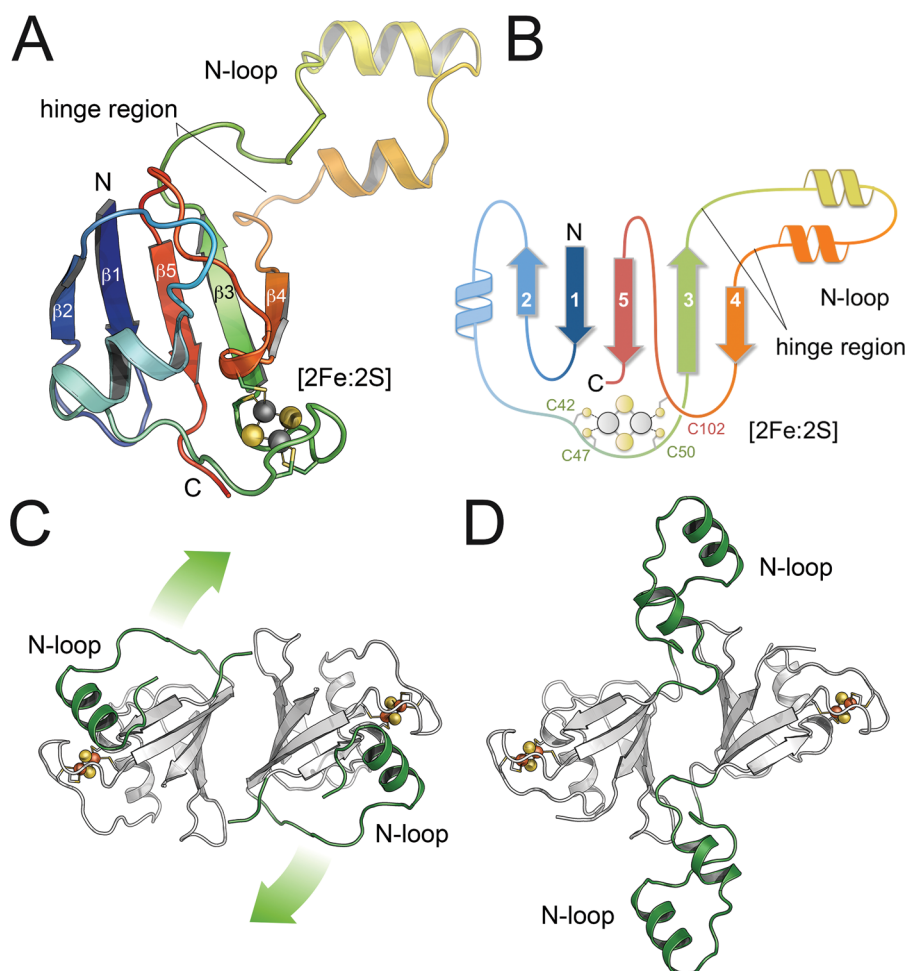


**Figure 2.** Three-dimensional structure of FeSII. (A) Cartoon representation of FeSII in the *open* state, as observed in four of the five copies present in the asymmetric unit. The functional N-loop is extended and well-defined. (B) The structural core of FeSII is a twisted  $\beta$ -sheet with 2–1–5–3–4 topology. The  $[2\text{Fe}:2\text{S}]$  cluster is coordinated by three cysteines (C42, C47, C50) from the loop connecting sheets  $\beta 2$  and  $\beta 3$ , and a fourth ligand from the loop connecting sheets  $\beta 4$  and  $\beta 5$  (C102). The main difference to other adrenodoxin-like ferredoxins lies in an extended *hinge region* that conveys flexibility to the N-loop. (C) One of five monomers in the asymmetric unit was in a *closed* conformation, with the N-loop folded back to shield the  $[2\text{Fe}:2\text{S}]$  cluster. The dimer shown was formed through a crystallographic 2-fold axis. (D) In contrast, the *open* state of FeSII (in identical orientation as in C) has extended N-loops, creating a putative interaction surface with nitrogenase and making the  $[2\text{Fe}:2\text{S}]$  cluster accessible.

5C). However, after 20 min of  $\text{O}_2$  exposure under *in vitro* conditions, FeSII in a final stoichiometric ratio of MoFe:FeSII of 1:1 was sufficient to retain 70% of acetylene reduction activity (Figure 1D). Higher ratios did not improve this further (Figure 1E). These results establish that FeSII not only protects nitrogenase (in particular Fe protein) by formation of a ternary complex as postulated previously,<sup>17</sup> but that MoFe protein and Fe protein themselves associate *in vitro* (and likely *in vivo*) into a complex that already shields Fe protein from the detrimental effects of  $\text{O}_2$ . Complex formation between MoFe and Fe proteins is transient, with association and dissociation during each electron transfer step at a rate of  $6\text{--}7\text{ s}^{-1}$  (for  $\text{H}_2$  production).<sup>18</sup> The protective effect of MoFe protein on Fe protein, however, indicates that dissociation may not be complete or that the associated state has a considerable lifetime.

**Three-Dimensional Structure of FeSII.** With cell constants of  $a = 133.3\text{ \AA}$ ,  $b = 134.5\text{ \AA}$  and  $c = 36.8\text{ \AA}$  and belonging to the orthorhombic space group  $P2_12_12$  (no. 18), the crystals obtained in the present work likely represent the same crystal form as those described by Moshiri and co-workers in 1994.<sup>17</sup>

Diffraction data were collected to  $2.1\text{ \AA}$  resolution, and the phase problem was solved by exploiting single-wavelength anomalous dispersion from the iron atoms of the  $[2\text{Fe}:2\text{S}]$  cluster. The crystals of FeSII contained five monomers per asymmetric unit, four of which formed two noncrystallographic dimers, while dimerization in the fifth monomer was mediated through the crystallographic 2-fold axis along *c*. *A. vinelandii* FeSII is a  $[2\text{Fe}:2\text{S}]$ -ferredoxin of the adrenodoxin-type, showing the canonical fold of plant and mammalian  $[2\text{Fe}:2\text{S}]$  ferredoxins with a twisted, five-stranded  $\beta$ -sheet of topology 2–1–5–4–3 (Figure 2A,B).<sup>19</sup> The metal cluster is coordinated by four cysteine residues, three of which (C42, C47, C50) originate from a typical  $\text{CX}_4\text{CX}_2\text{C}$  binding motif located in the loop region connecting strands 2 and 3 of the  $\beta$ -sheet. The fourth cysteine ligand to the cluster originates from the C-terminal part of FeSII (C102), forming part of the loop connecting strands 4 and 5 of the  $\beta$ -sheet. The cluster is located peripherally, on the outside of the half-barrel formed by the twisted  $\beta$ -sheet, making it accessible for the surrounding solvent (Figure 2A).

Unexpectedly, the five monomers of the protein that occupy the asymmetric unit of the crystal were not in identical

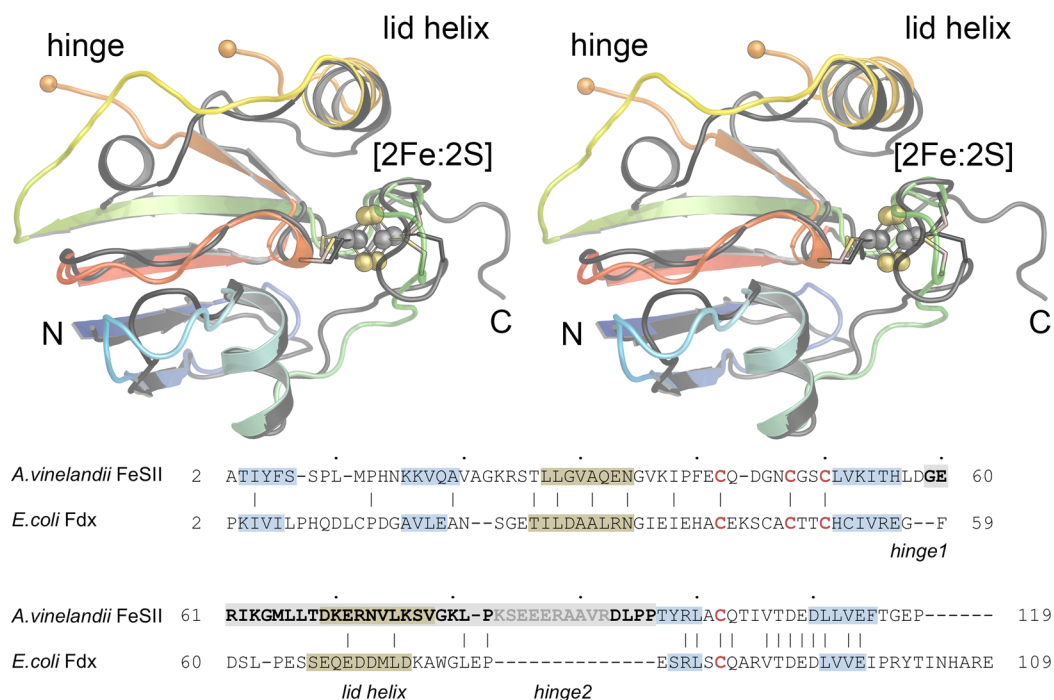


**Figure 3.** Structural superposition of the closed state of FeSII with the [2Fe:2S] ferredoxin (Fdx) from *E. coli* (PDB 1I7H). FeSII is colored from blue at the N-terminus to red at the C-terminus, while Fdx is shown in white. Both proteins are topologically equivalent, but FeSII contains insertions in two loops that constitute the hinge during transition to the open state. Eleven residues from K83–R92 were not defined in the electron density map. A structure-based sequence alignment of both proteins (23% sequence identity, below) shows that all secondary structure elements are conserved (cluster-binding Cys in red, strands blue, helices olive). The N-loop is highlighted in bold, with the disordered part of the closed state structure in gray.

conformations. Major structural differences were observed in an extended loop region (G59–P96) that makes up for more than 30% of the polypeptide chain and that we designated the N-loop (Figure 2A). The dimer of the one copy of FeSII that is generated through the crystallographic axis forms a compact globular domain with a partially disordered N-loop folded onto the protein (Figure 2C), showing an architecture that is similar to other ferredoxins of the family. Contrarily, in the four monomers that form two noncrystallographic dimers within the asymmetric unit, the N-loop is well-defined and attains an extended conformation that is directed 90° away from the adrenodoxin core of the protein, conveying a cross-shape to the dimer in what we hereafter all the *open* form (Figure 2D), while the more compact dimer represents a *closed* form. A DALI search<sup>20</sup> revealed a close structural kinship of FeSII with the [2Fe:2S] ferredoxin from *E. coli* (*EcFdx*) that has a putative role in iron–sulfur cluster biogenesis.<sup>21</sup> Although they only share 23% of sequence identity, the proteins are topologically equivalent (Figure 3). *EcFdx* strongly resembles the closed state of FeSII with a root-mean-squared deviation of 2.83 Å for all atoms, and both proteins share a conserved helix, the *lid helix* (T68–V78 in FeSII) that is positioned on top of the loop bearing the [2Fe:2S] cluster, thus effectively shielding it from the solvent. In a structure-based alignment, FeSII features two insertions with respect to *EcFdx*, one preceding and one following the lid helix (Figure 3). In transition to the open state, these insertions form the hinge at the base of the N-loop, so that the lid helix remains intact but is removed from the cluster.

**The [2Fe:2S] Cluster Environment in the Open and Closed States.** The iron–sulfur cluster of FeSII is located close to the protein surface and may thus be accessible both for

solvent and redox partners. In the closed state, however, the cluster is shielded on one side by the lid helix of the N-loop (Figure 4A). This is supported by two salt bridges (E71–R99 and D44–K70), while all other interactions are weaker van-der-Waals contacts.

When the protein transitions to the open state, the conformational change in the hinge region completely removes the lid helix from the proximity of the metal center, revealing a new protein surface and rendering the metal cluster far more accessible to the solvent (Figure 4B). While minor structural changes are also observed in the cluster-binding loop, it is the swinging out of the N-loop that fully transforms the appearance of FeSII from the closed to the open state (Figure 2C,D; 4C). During this transition, energy is required to break the E71–R99 and D44–K70 interactions, while at the same time reversibility is essential and no external energy source is available. This may be achieved by storing conformational energy (entropy) in the disordered loop region K83–R92 that in the open state forms a stable additional helix. This might explain the increased rigidity of the open form, in a mechanism similar to the movement of the LID domain in adenylate kinase.<sup>22</sup>

The presence of a [2Fe:2S] cluster in an oxygen-sensing protein and the variable conformations observed in the crystal structure suggest that the open and closed states are linked to the oxidized and reduced states of the iron–sulfur cluster, respectively. We have found both conformations (4 open monomers, 1 closed) in the same crystal that was obtained under oxic conditions from a partially reduced sample *as isolated*, while no crystals were obtained with fully reduced or fully oxidized protein. As iron–sulfur clusters typically achieve small reorganization energies by avoiding structural changes between oxidized and reduced states, a correlation of redox

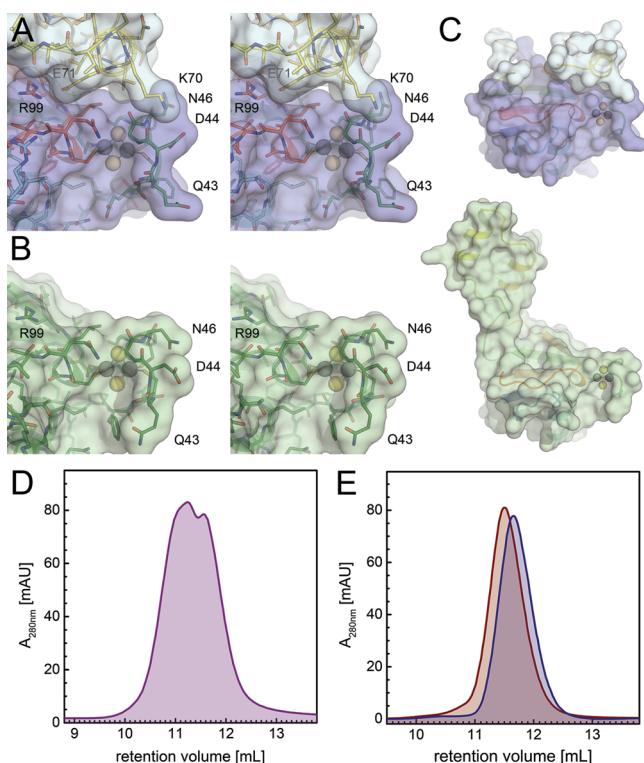


**Figure 4.** Iron–sulfur cluster environment in the closed (A) and open state (B) of FeSII (stereo images). The lid helix (residues T68–V78) that is positioned on top of the cluster-bearing loop is connected to the core domain of the protein through hydrogen bonds that include the interactions E71–R99 and D44–K70. In the open state (B) the solvent accessibility of the cluster is substantially increased. (C) A total view of the two states of FeSII in the same orientations as in (A) and (B) emphasizes the extent of the conformational change. (D) SEC-analysis of FeSII *as isolated* on Superdex 75, showing a double peak, indicating that the protein is purified as a mixture of two forms. (E) Successive SEC-analysis of fully oxidized (red) and fully reduced (blue) FeSII reveals a slightly increased apparent molecular mass for the oxidized form.

state and structure is not straightforward. However, FeSII *as isolated* was analyzed by size exclusion chromatography on Superdex 75, yielding a clear double peak that corresponded to two populations with different hydrodynamic radii (Figure 4D). Samples in the fully oxidized or reduced states, as confirmed by UV/vis spectroscopy, behaved as slightly shifted peaks in a chromatogram (Figure 4E), supporting that oxidation leads to an open form with a larger hydrodynamic volume. We conclude that the oxidation of the cluster is the cause of the conformational change observed in the crystal structure, with the oxidized state corresponding to the open form of the FeSII dimer.

We have proceeded to study the reoxidation of FeSII reduced with a stoichiometric amount of  $\text{Na}_2\text{S}_2\text{O}_4/\text{Tris}$  at pH 7.0 by molecular dioxygen (Figure 5A). As a reference, the same experiment was carried out with *Aquifex aeolicus* Fdx4, a dimeric  $[2\text{Fe}:2\text{S}]$  ferredoxin that is not related to the nitrogenase system (Figure 5A, inset).<sup>23</sup> Both proteins are fully reoxidized within several minutes upon addition of oxygen to the gas space of the cuvette. However, while the time course of reoxidation for Fdx4 shows the hyperbolic behavior of a first-order reaction and is completed within 10 min, the reoxidation of FeSII is 3-fold slower.

It also shows a sigmoidal time course that can be fitted with a Hill coefficient of 3 (Figure 5B), indicative of substantial intersubunit cooperativity. The cooperative behavior results in a steeper transition from reduced to oxidized state, making FeSII react more precisely than the noncooperative Fdx4. It further implies that the two protomers of a dimer will oxidize simultaneously. If oxidation leads to the transition to the open state, both N-loops will extend in unison and the protein can then bind to nitrogenase. Notably, in a nitrogenase assay carried out under reducing conditions and in the absence of  $\text{O}_2$ , the presence of FeSII has no effect on the obtained activities (Figure 5C). In contrast, activated FeSII protein was found to form a complex that we analyzed by analytical size exclusion chromatography on Superose 6 (Figure 5D), yielding a single peak of 320 kDa that is very well in line with a calculated composition of one MoFe heterotrimer, one Fe protein dimer and one dimer of FeSII (319 kDa).

**Dimer Formation and the Hinge Region.** In line with earlier studies, analytical size exclusion chromatography as well as the 3D structures of the open and closed form showed FeSII to be a functional homodimer in solution,<sup>17</sup> and we confirmed this by analytical size-exclusion chromatography (Figure S1). At  $1001 \text{ \AA}^2$  the buried surface area of the dimer in the closed state comprises only 8.2% of the total protein surface area (Figure 6A). Upon transition to the open form the contact area between the protomers expands to  $1387 \text{ \AA}^2$ , or 10.6% of the total surface area, predominantly because the extension of the N-loop creates additional intersubunit contacts (Figure 6B). In the closed form, the oval dimer interface is centered on a hydrophobic patch consisting of residues L57, L112 and Y5 of both monomers. Two major sets of H-bonding interactions stabilize the peripheral part of the interface, with N14 forming a short hydrogen bond to the backbone oxygen of L57 (2.9 Å) of the other monomer. Residue D110 forms a 2.9 Å hydrogen bond to the hydroxyl group of Y5 in the other protomer, as well as a second H-bond of 3.0 Å to  $\text{N}_\epsilon$  of residue K16 in the other monomer (Figure 6C). In the open form of the dimer these two sets of three H-bonds are retained, and additional interactions are generated by the N-loop folding back onto the other protomer in the dimer. These include backbone H-bonds (N14–G59, P12–R61) as well as interactions involving side chains. Hereby, R61 and the K53–D93 link that are not found in the closed state play a central role (Figure 6D). Interestingly, an interaction of residue R92 with the C-terminus of the other monomer (E118) is only found on one side of each of the two open dimers in the crystal, resulting in a structural asymmetry that may be functionally significant. A further residue of interest is H56 that—while not forming side chain H-bonds in either conformation—undergoes a rotation of  $160^\circ$  in this transition. As in the open state it forms a cation- $\pi$  interaction with the guanidino group of R61, the residue might help to stabilize the closed state. FeSII was strongly functionally impaired when this residue was mutated.<sup>24</sup> The *hinge2*-region that is disordered in unactivated FeSII (Figure 3) becomes highly structured in the open state, forming a short  $\alpha$ -helix with extensive side-chain interactions within the extended N-loop. K70 and E71 form the only H-bonding interactions between the lid and the globular remainder of the protein in the closed state, suggesting that they might be instrumental in stabilizing this form. We have generated a K70A/E71A double variant to assess whether this exchange may be sufficient to lock the protein in a constitutively open state that always inhibits nitrogen fixation.

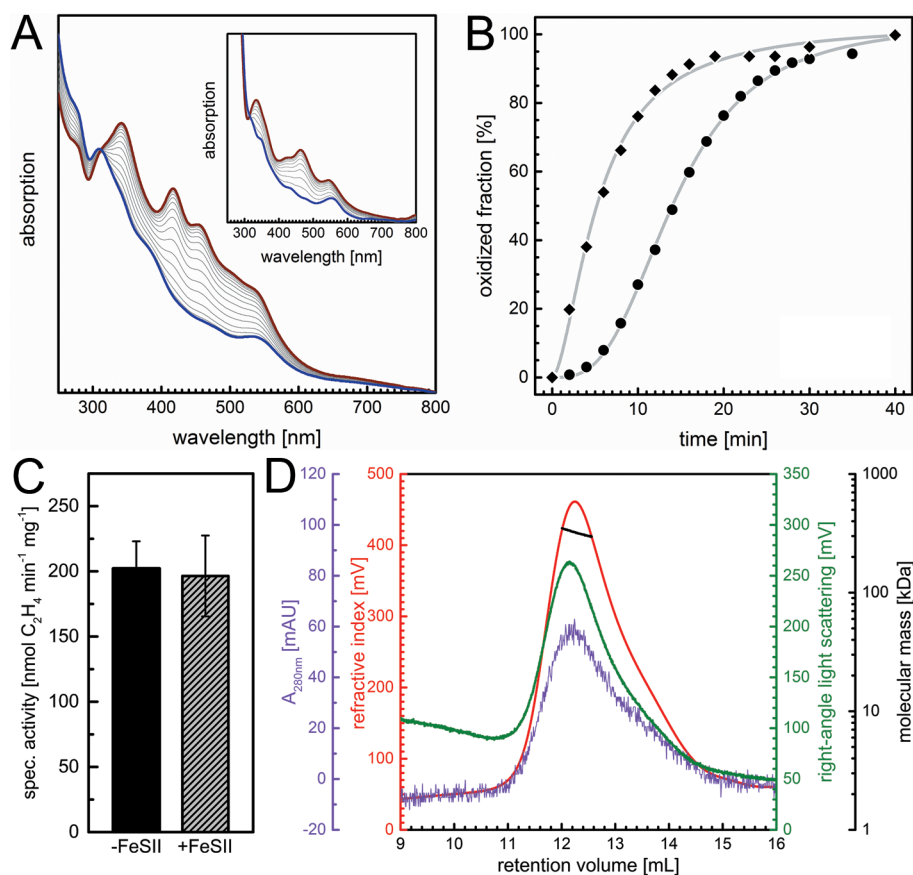


**Figure 5.** Oxidation of FeSII. (A) Upon exposure to air, reduced FeSII (blue) is reoxidized in vitro within approximately 20 min (red). The inset shows the same reoxidation for a reference protein, the dimeric thioredoxin-like [2Fe:2F] ferredoxin Fdx4 from *A. aeolicus*. (B) While the time-course of the reoxidation of Fdx4 (464 nm,  $\blacklozenge$ ) followed first-order kinetics, the reaction of FeSII with  $O_2$  (454 nm,  $\bullet$ ) was not only slower, but it showed a sigmoidal trace that is indicative of cooperativity within the dimer. The two monomers reoxidize in a concerted manner. (C) Under strict exclusion of dioxygen with a stoichiometric ratio of MoFe protein:Fe protein of 1:2,  $C_2H_4$  reduction activity is independent of the presence of the FeSII protein. In the absence of  $O_2$ , FeSII thus is in an inactive conformation that does not interfere with nitrogenase catalysis. (D) Analytical size-exclusion chromatography of the resulting  $\alpha_2\beta_2$ -MoFe: $\gamma_2$ -Fe:FeSII<sub>2</sub> complex, as a single peak with a molecular mass determined to 320 kDa.

However, this variant instead fully lost its protective function (data not shown), so that we conclude that residues K70, and in particular E71 that is fully buried in the closed state, are directly involved in the interaction with nitrogenase in the open state. This not only provides evidence that the open state is the one to actually interact with the enzyme, but it also helps to define the actual binding interface.

## DISCUSSION

In order to fulfill its role as an “oxygen chaperone” for nitrogenase, the FeSII protein must be able to quickly respond to the presence of dioxygen or a change in the redox status of the cytoplasm. It requires an  $O_2$ -dependent activation mechanism that allows for the formation of a tight, ternary complex with both MoFe protein and Fe protein of nitrogenase to attain an inactive but oxygen-tolerant state until the redox status of the cytoplasm returns to uncritical values. Complex formation is then reversed, so that nitrogenase catalysis can resume.

Here we have shown that FeSII exists in two conformational states that relate to oxidation states of the cluster (Figure 4D,E) and that the oxidative activation of the cluster occurs cooperatively in both monomers of the stable dimer of FeSII (Figure 5). In the open form, FeSII forms a complex with MoFe and Fe protein in a defined stoichiometry (Figure 5D).

The obvious question then is how the ternary complex is constructed. While an experimental structure is not available at this point, several lines of evidence can be integrated into a hypothetical model.

The increased oxygen tolerance of Fe protein exhibited in the presence of MoFe protein even without FeSII (Figure 1C) indicates that the two component proteins at most times are present in a complex in the cell, and in this state the Fe protein is already markedly stabilized. We can then hypothesize that FeSII comes into the picture only later in evolution, conveying additional protection in high-oxygen environments. A first complex structure for nitrogenase MoFe and Fe protein was presented in 1996, stabilized with  $ADP\cdot AlF_4^-$ , a transition state mimic for ATP-hydrolyzing enzymes. Here the C2 axis of the Fe protein dimer coincides with the 2-fold pseudosymmetry axis connecting the evolutionarily related  $\alpha$ - and  $\beta$ -subunits of MoFe protein, situated right above P-cluster.<sup>25</sup> Following up on this work, Tezcan and Rees found that depending on the nucleotide-loading of Fe protein the two proteins can form various complexes,<sup>26</sup> also possibly with an asymmetric loading of Fe protein with nucleotide.<sup>27</sup> Most recently, the functional relevance of these variations in complex formation was shown,<sup>28</sup> and one of the observed complexes may be of particular interest in the present context. Initially grown from a mixture of MoFe protein and Fe protein in the absence of

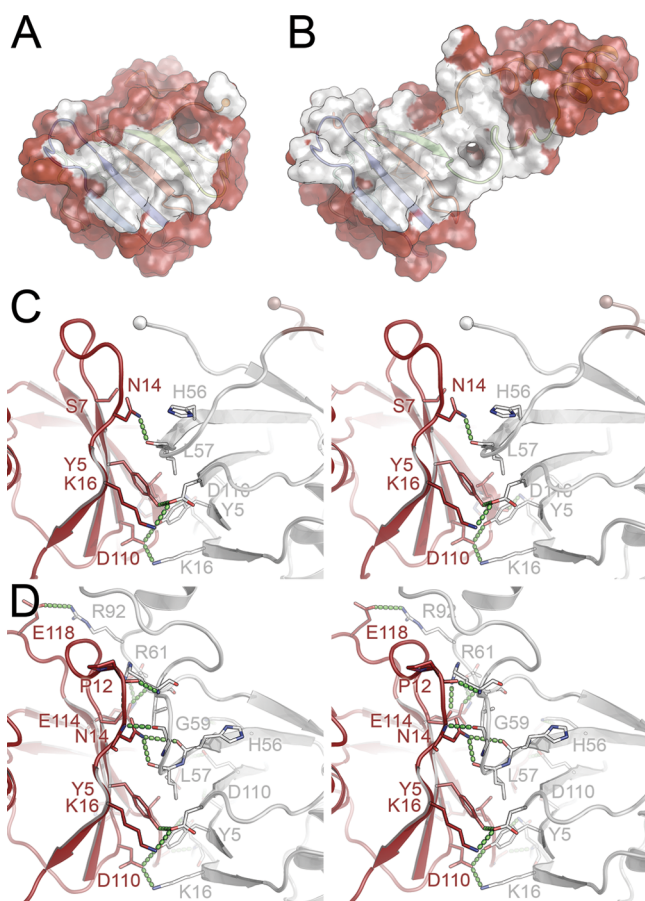


**Figure 6.** Dimerization interface of FeSII. (A) In the closed state, the interaction surface of the dimer covers 8.2% of the surface of a monomer. (B) The extension of the N-loop upon opening of the protein enlarges the dimerization interface to 10.6%. (C) Stereo representation of the interface in the closed state. Three H-bonds—doubled through dimerization—form the main contacts. (D) In the open state, the N-loop enters multiple additional interactions, stabilizing the quaternary structure.

nucleotides, an asymmetric complex was formed where Fe protein is shifted from its optimal binding position and largely interacts with one  $\gamma$ -protomer on the  $\beta$ -subunit only. This complex is peculiar, as the increased intercluster distance renders it incompetent for electron transfer. However, it closely juxtaposes residues K400 $\beta$  and E112 $\gamma$  that can be specifically cross-linked under turnover conditions with 1-ethyl-3-[3-(dimethylamino)-propyl] carbodiimide (EDC),<sup>29–31</sup> indicating that this complex indeed exists *in vivo*. Its role in catalysis is unclear, but it was suggested to represent a first encounter complex of the two components.<sup>31</sup> Tezcan and co-workers most recently obtained this complex also in the presence of ATP and ADP and described that the Fe protein attains a more open conformation than in the transition state complex with ADP·AlF<sub>4</sub><sup>−</sup> or AMPPCP.<sup>28</sup>

Complex formation in nitrogenase is largely determined by electrostatic interactions, setting the system apart from other electron transfer interactions that are characterized by short-lived, transient encounter complexes.<sup>32</sup> Nitrogenase activity decreases with increasing concentrations of NaCl when this electrostatic interaction is disturbed,<sup>28</sup> and we have consequently investigated the influence of NaCl on the O<sub>2</sub>-protection by FeSII. Both in the absence and presence of O<sub>2</sub>

the loss of nitrogenase activity showed a linear dependence on NaCl concentration (Figure S2). Without oxygen, nitrogenase activity decreased at a rate of 0.53%·mM<sup>−1</sup>, reflecting the effect of increasing ionic strength on the interaction of the components as described previously.<sup>28</sup> When the assay was repeated after exposing the mixture to 10% O<sub>2</sub> for 10 min in the presence of FeSII, the obtained activity was reduced to 50% at 0 mM NaCl due to the detrimental effects of O<sub>2</sub> on Fe protein. When NaCl concentrations were increased at unchanged exposure times to oxygen, the remaining activity decreased at a higher rate of 0.90%·mM<sup>−1</sup>. In addition to affecting the interaction of MoFe protein and Fe protein, NaCl thus had a negative effect on the binding of FeSII to form an oxygen-insensitive state. This confirms that the interaction of FeSII with nitrogenase is also ionic by nature. While both nitrogenase components show a distinctly negative electrostatic surface potential,<sup>31,33</sup> the FeSII protein carries a complementary, positive charge that is unusual for ferredoxins and is also reflected by its binding to a cation exchanger material during isolation.

A further piece of information is that—as mentioned above—our initial tests with His<sub>6</sub>-tagged FeSII showed no protection of nitrogenase. A possible explanation for this is that the affinity tag was placed in a position where it directly interferes with the interaction of activated (open) FeSII with the preformed MoFe-Fe protein complex. This places the possible interaction surface of FeSII right into one concave edge of the dimer, and with a distance of 44 Å for the C-termini it further implies that the interaction sides within one dimer either cover the entire inner surface of the protein or are on opposing sides.

Finally, we observe maximal protection of nitrogenase by FeSII at a stoichiometric ratio of MoFe:FeSII of 1:1. This leads to the interesting implication that a single FeSII dimer cannot protect the two distant docking sites for Fe protein on MoFe protein. In the complexes of MoFe protein and Fe protein, two Fe protein dimers interact with MoFe protein on opposing sides, in proximity to the two P-clusters, respectively. An exception to this stoichiometry was found earlier by Eady and co-workers, when working on hybrid complex formation between *A. vinelandii* MoFe protein and *C. pasteurianum* Fe protein.<sup>35</sup> The authors investigated H<sub>2</sub> evolution and found a functional role for a 1:1 complex of both proteins, similar to the one observed by Tezcan and Rees.<sup>26</sup>

Taken together, a possible model that emerges is that this asymmetric complex of MoFe protein and Fe protein (designated *DGI* by Tezcan and co-workers<sup>28</sup>) represents not only a transient encounter complex, but a more persistent association of the two proteins, in which MoFe protein already exerts a protective effect on the highly labile Fe protein. This complex is then further stabilized by activated (open) FeSII. Given the location of the C-terminus and the protein surface that is generated only upon opening of the N-loop we generated a set of restrictions for the HADDOCK docking server that yielded a model with one monomer of FeSII fitting the crevice between MoFe protein and the asymmetrically bound Fe protein very well (Figure 7).<sup>34</sup> This complex would have a predicted molecular mass of 319 kDa, in accordance with our SEC-RALS data (Figure 5D). FeSII inserts deeply into the cleft between the two enzyme components, but leaving the [2Fe:2S] cluster accessible to the solvent, ready for inactivation by reduction. While this model is hypothetical, it is noteworthy that the possible interaction of a ferredoxin in the cleft of the

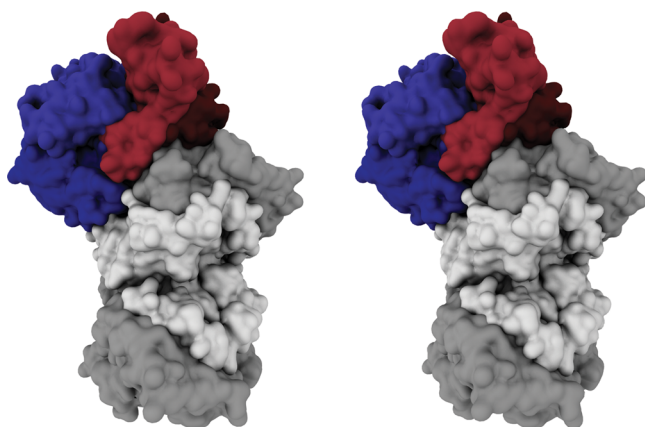


**Figure 7.** Hypothetical interaction model for FeSII with the nitrogenase complex (stereo image). On the basis of restraints from surface electrostatics, the determined interaction stoichiometry and the inactivity of the K70/E71 variant, a binding model was generated and geometry optimized using HADDOCK.<sup>34</sup> One dimeric FeSII protein (red) stabilizes an asymmetric complex of MoFe protein (gray) and Fe protein (blue). The interaction surface of FeSII is formed by both monomers and only exists in the open state.

DGI state might also imply that reduction of Fe protein during catalysis (by a ferredoxin or flavodoxin) may be feasible without complete dissociation of the two components.

In summary, the unexpected conformational flexibility of FeSII that was observed in the crystal structure implies an oxygen-dependent, concerted activation mechanism of the dimeric ferredoxin that allows for complex formation with a preformed and partially stabilizing MoFe/Fe protein complex in the cytoplasm of the diazotroph *A. vinelandii*. Further studies will be required to decide whether the iron–sulfur cluster of FeSII plays an active role in the protection of nitrogenase or simply represents a redox-driven conformational switch that allows for a complex formation driven by surface complementarity and electrostatics. It seems, however, evident that the protective effect of FeSII may be of high value for the numerous ongoing attempts in different laboratories to refactor nitrogenase or obtain recombinant expression in a non-diazotrophic host.<sup>36,37</sup>

## MATERIALS AND METHODS

**Cultivation of *Azotobacter vinelandii* and Isolation of Nitrogenase.** *A. vinelandii* (DSM2289)<sup>38</sup> was grown in modified Burke's medium (pH 7.8) in an air atmosphere.<sup>10</sup> A nitrogen-containing (10 mM NH<sub>4</sub>Cl) preculture of 100 mL was used to inoculate main cultures of 500 mL that contained only 1.3 mM of NH<sub>4</sub>Cl as the sole nitrogen source. This resulted in derepression of nitrogenase gene expression upon ammonium depletion. Cells were harvested by centrifugation at an optical density (OD<sub>600 nm</sub>) of 2.5 and washed with 50 mM Tris/HCl buffer at pH 7.4. All subsequent steps were carried out anoxically using modified Schlenk techniques. All buffers were degassed by repeated cycles of vacuum and N<sub>2</sub>, and supplemented with 2.5 mM Na<sub>2</sub>S<sub>2</sub>O<sub>4</sub> adjusted to pH 7.5. Cells were disrupted with an Emulsiflex homogenizer (Avestin) in an N<sub>2</sub> atmosphere. The lysate was centrifuged at 100 000×g for 30 min and the supernatant was loaded onto a HiTrap Q anion exchange column (GE Healthcare) pre-equilibrated with 50 mM Tris/HCl buffer at pH 7.4. MoFe protein and Fe protein were eluted with a linear NaCl gradient, with MoFe protein eluting at 190 mM, followed by Fe protein at 370 mM. The concentrated proteins were loaded onto a size exclusion column (S200, 26/60, GE Healthcare) equilibrated with 100 mM NaCl, 20 mM Tris/HCl buffer at pH 7.4. Pure MoFe and Fe

proteins were concentrated with a Vivaspin concentrator (100 000 kDa and 30 000 kDa MWCO, Sartorius) under 5 bar N<sub>2</sub> pressure.

**Protein Production and Isolation.** The open reading frame for FeSII of *A. vinelandii* (AVIN\_39700) was obtained as a synthetic gene (GeneArt) and inserted into the multiple cloning site of a pET21a expression vector (Novagen) by Gibson assembly.<sup>39</sup> For protein production, chemically competent *E. coli* BL21 (DE3) C43 cells were transformed with the vector.<sup>40</sup> The cells were cultivated in Luria–Bertani medium supplemented with 100 μg·L<sup>-1</sup> of ampicillin, and gene expression was induced by the addition of isopropyl-thiogalactoside to a final concentration of 0.2 mM when an OD<sub>600 nm</sub> of 0.6 was reached. The cells were harvested by centrifugation 4 h after induction, resuspended in 50 mM sodium acetate buffer at pH 5.2 and disrupted by three passages through a microfluidizer at 100 MPa (Microfluidics). After removal of cell debris by centrifugation, the FeSII protein was purified by cation exchange chromatography on a HiTrap SP column with 5 mL bed volume (GE Healthcare) that was developed with a linear gradient of from 0–100 mM of NaCl. Fractions containing FeSII were pooled and concentrated by ultrafiltration, to be subsequently applied to size exclusion chromatography on Superdex 75 (GE Healthcare), yielding a single, symmetric peak corresponding to a dimer of the protein.

**Analytical Size-Exclusion Chromatography.** Characterizations of FeSII in various redox states and of the complex formed with the nitrogenase components was carried out by size-exclusion chromatography using a Superdex 75 10/300 column (GE Healthcare) on a Viscotek triple detector away (Malvern) with detection of UV/vis absorption, refractive index and right-angle light scattering, allowing for the absolute determination of the hydrodynamic radius (or the apparent molecular weight) of the sample.

**Nitrogenase Protection and Activity Assays.** Nitrogenase activity was monitored by following a nonphysiological side reaction, the reduction of acetylene to ethylene that can straightforwardly be quantified by gas chromatography. In a 10 mL Wheaton vial, 1 mL of reaction mixture was sealed under an Ar atmosphere. The mixture contained 0.65 nmol of MoFe protein (α<sub>2</sub>β<sub>2</sub>-heterotetramer) and/or 1.3 nmol of Fe protein (dimer) and—if applicable—1.3 nmol of FeSII (dimer), as well as 0.125 g·L<sup>-1</sup> of phosphocreatine kinase, 15 mM of phosphocreatine, 2.5 mM ATP, 5 mM MgCl<sub>2</sub>, and 20 mM of Tris/HCl buffer at pH 7.4. To this mixture, 0.2 mL of O<sub>2</sub> were added via a gastight syringe to a final concentration of 2% O<sub>2</sub>, 98% Ar and incubated for variable times. Oxygen was then removed by flushing the headspace with 100% Ar, and to avoid its decomposition in the presence of oxygen, Na<sub>2</sub>S<sub>2</sub>O<sub>4</sub> was added to a final concentration of 2.5 mM only after this step. For the assay, the respective missing components were added and 1 mL of C<sub>2</sub>H<sub>2</sub> was injected to the gas space with a gastight syringe and the reaction was allowed to proceed for 3 min, before a sample of 1 mL of headspace was taken and injected into a gas chromatograph for the quantification of ethylene. Note that the acetylene reduction assay is commonly carried out with a large excess of Fe protein. Here we used a stoichiometric ratio of MoFe protein (tetramer) to Fe protein (dimer) of 1:2 in order to investigate the action of FeSII, leading to lower specific activities. In *A. vinelandii* cells, the MoFe:Fe protein ratio was determined to 1–2,<sup>41,42</sup> so that our conditions are closer to the physiological situation than the ratio of 1:20–40 that is commonly used in acetylene reduction assays.

**Structure Determination of FeSII.** *A. vinelandii* FeSII was crystallized using sitting-drop vapor diffusion. Crystals were not obtained from either fully oxidized or fully reduced samples, but only in a partly reduced state as isolated. Small, three-dimensional crystals were obtained by mixing 0.5 μL of protein solution (50 g·L<sup>-1</sup>) with the same volume of a reservoir solution containing 1 M of trisodium citrate and 0.01 M sodium tetraborate (Na<sub>2</sub>B<sub>4</sub>O<sub>7</sub>) at pH 8.0. After 4 days, crystals were harvested, mounted in a nylon loop and flash-cooled in liquid nitrogen. Diffraction data were collected on beamline X06DA at the Swiss Light Source (Paul-Scherrer-Institut, Villigen, CH), using a Pilatus 2M detector. 360° of data were collected with 0.5° oscillations per image. Reflections were recorded to below 2.2 Å resolution at an X-ray wavelength of 1.0 Å. For phase determination, a



further data set was collected on the iron K-edge at a wavelength of 1.729 Å. The data were indexed and integrated with XDS,<sup>43</sup> and using the Fe K-edge peak data set the phase problem was solved by single-wavelength anomalous dispersion using AutoSol of the PHENIX suite.<sup>44</sup> We located 10 Fe sites belonging to the [2Fe:2S] clusters of 5 monomers of FeSII in the asymmetric unit. The structural model was built with COOT<sup>45</sup> and refined with REFMAC5.<sup>46</sup> Figures were generated using PyMOL (Schrödinger LLC) and Maya (Autodesk). Data collection and refinement statistics are summarized in Supporting Table S1.

## ■ ASSOCIATED CONTENT

### ● Supporting Information

The Supporting Information is available free of charge on the ACS Publications website at DOI: 10.1021/jacs.5b10341.

Supporting Figures S1 and S2; Data collection and refinement statistics table (PDF)

## ■ AUTHOR INFORMATION

### Corresponding Author

\*einsle@biochemie.uni-freiburg.de

### Notes

The authors declare no competing financial interest.

## ■ ACKNOWLEDGMENTS

We thank the beamline staff at the Swiss Light Source (Villigen, CH) for excellent support during data collection. This work was supported by Deutsche Forschungsgemeinschaft (RTG 1976 and EI-520/5) and the European Research Council (ERC grant no. 310656). Coordinates and experimental structure factor amplitudes have been deposited with the Protein Data Bank (<http://www.pdb.org>) with the accession code 5FFI.

## ■ REFERENCES

- (1) Canfield, D. E.; Glazer, A. N.; Falkowski, P. G. *Science* **2010**, *330*, 192.
- (2) Howard, J. B.; Rees, D. C. *Proc. Natl. Acad. Sci. U. S. A.* **2006**, *103*, 17088.
- (3) Schubert, S. *Fert. Res.* **1995**, *42*, 99.
- (4) Robson, R. L.; Postgate, J. R. *Annu. Rev. Microbiol.* **1980**, *34*, 183.
- (5) Yates, M. G. In *The Nitrogen and Sulphur Cycles*; Cole, J. A., Ferguson, S. J., Eds.; Cambridge University Press: Cambridge, 1988; p 383.
- (6) Dalton, H.; Postgate, J. R. *J. Gen. Microbiol.* **1968**, *54*, 463.
- (7) Gallon, J. R. *New Phytol.* **1992**, *122*, 571.
- (8) Seefeldt, L. C.; Hoffman, B. M.; Dean, D. R. *Annu. Rev. Biochem.* **2009**, *78*, 701.
- (9) Georgiadis, M. M.; Komiyama, H.; Chakrabarti, P.; Woo, D.; Kornuc, J. J.; Rees, D. C. *Science* **1992**, *257*, 1653.
- (10) Spatzal, T.; Aksoyoğlu, M.; Zhang, L. M.; Andrade, S. L. A.; Schleicher, E.; Weber, S.; Rees, D. C.; Einsle, O. *Science* **2011**, *334*, 940.
- (11) Kim, J. S.; Rees, D. C. *Nature* **1992**, *360*, 553.
- (12) Einsle, O.; Tezcan, F. A.; Andrade, S. L. A.; Schmid, B.; Yoshida, M.; Howard, J. B.; Rees, D. C. *Science* **2002**, *297*, 1696.
- (13) Einsle, O. *JBIC, J. Biol. Inorg. Chem.* **2014**, *19*, 737.
- (14) Shethna, Y. I.; Dervartanian, D. V.; Beinert, H. *Biochem. Biophys. Res. Commun.* **1968**, *31*, 862.
- (15) Bulen, W. A.; LeCompte, J. R. *Methods Enzymol.* **1972**, *24*, 456.
- (16) Robson, R. L. *Biochem. J.* **1979**, *181*, 569.
- (17) Moshiri, F.; Crouse, B. R.; Johnson, M. K.; Maier, R. J. *Biochemistry* **1995**, *34*, 12973.
- (18) Hageman, R. V.; Burris, R. H. *Proc. Natl. Acad. Sci. U. S. A.* **1978**, *75*, 2699.
- (19) Grinberg, A. V.; Hannemann, F.; Schiffler, B.; Müller, J.; Heinemann, U.; Bernhardt, R. *Proteins: Struct., Funct., Genet.* **2000**, *40*, 590.
- (20) Holm, L.; Sander, C. *J. Mol. Biol.* **1993**, *233*, 123.
- (21) Kakuta, Y.; Horio, T.; Takahashi, Y.; Fukuyama, K. *Biochemistry* **2001**, *40*, 11007.
- (22) Müller, C. W.; Schlauderer, G. J.; Reinstein, J.; Schulz, G. E. *Structure* **1996**, *4*, 147.
- (23) Yeh, A. P.; Ambroggio, X. I.; Andrade, S. L. A.; Einsle, O.; Chatelet, C.; Meyer, J.; Rees, D. C. *J. Biol. Chem.* **2002**, *277*, 34499.
- (24) Lou, J. R.; Moshiri, F.; Johnson, M. K.; Lafferty, M. E.; Sorokin, D. L.; Miller, A. F.; Maier, R. J. *Biochemistry* **1999**, *38*, 5563.
- (25) Schindelin, N.; Kisker, C.; Sehlessman, J. L.; Howard, J. B.; Rees, D. C. *Nature* **1997**, *387*, 370.
- (26) Tezcan, F. A.; Kaiser, J. T.; Mustafa, D.; Walton, M. Y.; Howard, J. B.; Rees, D. C. *Science* **2005**, *309*, 1377.
- (27) Tezcan, F. A.; Kaiser, J. T.; Howard, J. B.; Rees, D. C. *J. Am. Chem. Soc.* **2015**, *137*, 146.
- (28) Owens, C. P.; Katz, F. E.; Carter, C. H.; Luca, M. A.; Tezcan, F. A. *J. Am. Chem. Soc.* **2015**, *137*, 12704.
- (29) Willing, A.; Howard, J. B. *J. Biol. Chem.* **1990**, *265*, 6596.
- (30) Willing, A. H.; Georgiadis, M. M.; Rees, D. C.; Howard, J. B. *J. Biol. Chem.* **1989**, *264*, 8499.
- (31) Schmid, B.; Einsle, O.; Chiu, H. J.; Willing, A.; Yoshida, M.; Howard, J. B.; Rees, D. C. *Biochemistry* **2002**, *41*, 15557.
- (32) Bashir, Q.; Volkov, A. N.; Ullmann, G. M.; Ubbink, M. J. *Am. Chem. Soc.* **2010**, *132*, 241.
- (33) Schmid, B.; Ribbe, M. W.; Einsle, O.; Yoshida, M.; Thomas, L. M.; Dean, D. R.; Rees, D. C.; Burgess, B. K. *Science* **2002**, *296*, 352.
- (34) De Vries, S. J.; van Dijk, M.; Bonvin, A. M. J. *J. Nat. Protoc.* **2010**, *5*, 883.
- (35) Clarke, T. A.; Maritano, S.; Eady, R. R. *Biochemistry* **2000**, *39*, 11434.
- (36) Wang, L. Y.; Zhang, L. H.; Liu, Z. Z.; Zhao, D. H.; Liu, X. M.; Zhang, B.; Xie, J. B.; Hong, Y. Y.; Li, P. F.; Chen, S. F.; Dixon, R.; Li, J. L. *PLoS Genet.* **2013**, *9*, e1003865.
- (37) Temme, K.; Zhao, D. H.; Voigt, C. A. *Proc. Natl. Acad. Sci. U. S. A.* **2012**, *109*, 7085.
- (38) Lipman, J. G. *Rep. New Jersey Agric. Exp. Stat.* **1903**, *24*, 217.
- (39) Gibson, D. G.; Young, L.; Chuang, R. Y.; Venter, J. C.; Hutchison, C. A.; Smith, H. O. *Nat. Methods* **2009**, *6*, 343.
- (40) Miroux, B.; Walker, J. E. *J. Mol. Biol.* **1996**, *260*, 289.
- (41) Jacobs, D.; Mitchell, D.; Watt, G. D. *Arch. Biochem. Biophys.* **1995**, *324*, 317.
- (42) Klugkist, J.; Haaker, H.; Wassink, H.; Veeger, C. *Eur. J. Biochem.* **1985**, *146*, 509.
- (43) Kabsch, W. *Acta Crystallogr., Sect. D: Biol. Crystallogr.* **2010**, *66*, 125.
- (44) Adams, P. D.; Afonine, P. V.; Bunkoczi, G.; Chen, V. B.; Echols, N.; Headd, J. J.; Hung, L. W.; Jain, S.; Kapral, G. J.; Kunstleve, R. W. G.; McCoy, A. J.; Moriarty, N. W.; Oeffner, R. D.; Read, R. J.; Richardson, D. C.; Richardson, J. S.; Terwilliger, T. C.; Zwart, P. H. *Methods* **2011**, *55*, 94.
- (45) Emsley, P.; Lohkamp, B.; Scott, W. G.; Cowtan, K. *Acta Crystallogr., Sect. D: Biol. Crystallogr.* **2010**, *66*, 486.
- (46) Murshudov, G. N.; Skubak, P.; Lebedev, A. A.; Pannu, N. S.; Steiner, R. A.; Nicholls, R. A.; Winn, M. D.; Long, F.; Vagin, A. A. *Acta Crystallogr., Sect. D: Biol. Crystallogr.* **2011**, *67*, 355.